HIGH-PRESSURE HELIUM-3 SCINTILLATION POSITION-SENSITIVE DETECTOR OF THERMAL NEUTRONS

A. Bolozdynya[1], A. Bolotnikov, J. Richards
Constellation Technology Corporation, 7887 Bryan Dairy Rd., Largo, FL 33777

Abstract

The objective of this study is to demonstrate the feasibility of constructing a compact neutron detector that is sensitive to thermal and epithermal neutrons and has high rejection efficiency relative to gamma-ray background. A two-channel high-pressure ^{3}He scintillation detector is considered for the detection of neutrons in coincidence mode. The detector consists of two large avalanche photodiodes viewing a gas volume filled with pressurized ^{3}He. Experiments with the detector demonstrate high efficiency to neutrons and high rejection ability to gamma rays. Position sensitivity of the detector to thermal neutrons is demonstrated and confirmed with computer simulations.

1. Introduction

Real-time personal neutron dosimeters are required for occupational radiation protection at nuclear power plants, nuclear material processing facilities, high-energy particle accelerators, high-altitude flights, and long-term space missions [1]. There is a great interest in the detection of thermal neutrons for oil well logging [2] and on-site nuclear monitoring [3]. For decades, the most popular instruments for measuring thermal neutron fluxes have been gas proportional counters [2, 4-6]. However, only relatively low gas (^{3}He or BF_3) pressure (a few bars) can be used in proportional counters because of technical limitations in the application of sufficiently high voltages for effective charge amplification. That reduces the efficiency of the detectors to epithermal neutrons.

One recently investigated detector technique uses a silicon PIN photodiode with a gadolinium-foil converter [1]. The converter emits several conversion electrons with energies between 29 keV and 246 keV and gamma-rays in the range of >231 keV per single neutron capture. This method needs simultaneous measurements of electrons and gammas and subtraction of the effect from gamma-interactions. That makes the technique complicated and sensitive to the calibration procedure utilized. The gadolinium foil should be thinner than 25 microns to make electrons effectively escape from the foil. With a 1 cm^2 sensitive area, the detector has an efficiency of 5.6% at ideal conditions. The gadolinium target has no significant advantages for detection of fast neutrons.

Twenty years ago [12,13], here were several attempts to use high-pressure ^{3}He and ^{4}He gas scintillators for detection of fast neutrons. In those works, photomultipliers were used as photo-receivers that introduced a certain limit on the pressure of the gas and made the whole design very fragile. Another approach to use solid state photodiodes mounted directly inside a high-pressure gas chamber was investigated in this work.

[1] Corresponding author; e-mail bolozdynya@contech.com

2. Methods

Scintillation detectors have several advantages compared to other ionization detectors: no high voltage bias is required; much higher pressure can be used for the fast signals for time measurements; fewer electronic readout channels working in coincidence mode; capability to reject background.

Thermal neutrons are effectively absorbed in ^{3}He, yielding a triton and proton, which share the reaction energy of 764 keV plus the kinetic energy of the incident neutron (actually, negligible for thermal neutrons). The proton and triton expend their energy in the gas. The trapping cross-section of thermal neutrons is $s_{th}(^3\text{He})$ = 5,327 barns. At only 1 cm detector thickness and 20 atm pressure, the calculated efficiency is about 94%. In the range of the expected neutron signal (~764 keV), the intensity of natural gamma-ray background is at least an order of magnitude less than that in the working range of the reference detector. There is no artificial gamma-ray background from the ^{3}He target gas.

^{3}He has a relatively high cross-section of elastic interactions for fast neutrons [11]. Elastic scattering neutrons bounce ^{3}He atoms. The recoil atoms depositing their kinetic energy into the gas generate the scintillation. Detection efficiency for the fast neutrons is proportional to the helium pressure.

2.1. Range of Particles in Helium-3

According to semi-empirical calculations [9], the range of protons in helium is 8.8 10^{-4} g/cm^2. The density of natural and ^{3}He helium at normal conditions is r_{He4} = 0.1785 and 0.13 mg/cm^3, respectively. Hence, the range of protons in 20 bar ^{3}He may be estimated as L_p = (1/20)(8.8 10^{-4} g/cm^2)/(0.00013 g/cm^3) = 3.4 mm. (Another empirical formula for calculation of proton range in ^{3}He can be found in [2]: L_p = 2.4/p[bar] inches, which gives a similar range value). The range of protons in 100 bar ^{3}He will be about 0.7 mm. The range of triton will be about 3 times longer. In the case of elastic scattering fast neutrons, the range of ^{3}He recoils will be about 2 cm at 1 MeV and 6 cm at 10 MeV kinetic energy of recoils.

2.2. Wave Length Shifting

Helium scintillates in the VUV range. In order to measure the scintillation, a two-step wavelength shifting process has been used. First, a gas mixture of ^{3}He with 0.5% Xe was used that shifts He-atom emission into the 175 nm wavelength range typical for xenon. Secondly, all internal surfaces of the cell, including the optical window, were coated with 0.5 mg/cm^2 of vacuum deposited p-terphenyl, which effectively absorbs 175 nm photons and re-emits 350 nm photons with >90% quantum efficiency.

A wavelength shifting layer of 0.5 mg/cm^2 p-terphenyl is used to shift 170 nm scintillation photons to 400 nm photons detected in the photodetectors. According to [9], the range of 570 keV protons in carbon is about 1.17 mg/cm^2. Therefore, the protons generated in the gas as the result of neutron capture are able to penetrate the organic

coating and deposit the rest of their kinetic energy into the photodetectors directly. Note that the wavelength shifter will be scintillating under the influence of the protons passing through. The effect may return some part of the energy lost by the protons and tritons in the organic coating to the photodetectors.

2.3. Gas Purification

In order to achieve a high light output of the scintillation at high pressure, the gas should be carefully purified from any molecular impurities. A purification system based on molecular sieves cooled down to 77 K has been developed and constructed. Our preliminary experiments with PMT have shown that pure He+0.5% Xe gas mixture exhibits a decay time of about 200 nsec. The duration of scintillations serves as a signature for the purity of the gas. Gas contaminated with molecular impurities demonstrates lower light-output and shorter scintillation pulses. Observation of shorter decay times has been used as a sign of contamination of the gas with molecular impurities.

2.4. Detector

We have chosen 16-mm diameter silicone avalanche photodiodes of model SD7911 produced by Advanced Photonix, Inc. Preliminary studies confirm that their construction is clean and can be used in pressurized xenon and ^{3}He without changing gas purity (see below). The photodiodes provide a gain up to x 300. For calibration and equalization of photodiode responses with separate bias, we use a 450 nm LED BNC Light Pulse Generator, model 6010. The light pulse is introduced into the detector via a fiber cable attached to the small sapphire window. The window is between the photodiodes in such a way that diffusely reflected light illuminates both photodiodes with equal probability.

A compact two-channel high-pressure ^{3}He scintillation detector (HeSD) consists of two photodetectors with a 7 mm gap between them, mounted inside a stainless steel shell with ~1 mm and 1" diameter input windows. The gap is filled with ^{3}He (+0.1% Xe) gas under a pressure of 30 bar. No electric field is applied to the gap. A para-terphenyl (p-TP) wave-shifter with a thickness of 0.5 mg/cm^2 is deposited on the surfaces of the photodetectors. Due to the geometry selected for the detector, the magnitudes of the both signals (A1 and A2) should be approximately the same: A1 ≈ A2. This approach allows the detector to reject signals generated by interaction of radiation with the photodetectors and to arrange a so-called “wall-less” detector sensitive only to interactions occurring in the gas. ^{3}He itself has a very low cross-section of interaction with gamma-rays, thus making the detector insensitive to gamma-rays. The design of the two-channel HeSD with 2-photodiodes readout is shown in Fig. 1.

2.6. Electronics

In this project, we have used NIM electronics and a desktop computer with APTEC PCMCA/Super PC-based MCA card and APTEC software providing data acquisition, display, peak search, and analysis. The system includes a LeCroy LT346L digital scope

for signal shape analyses. Miniature charge-sensitive Cremat CR-101D preamplifiers are DC coupled to the photodiodes. The preamplifiers provide fast rise time and perform with low noise. A block diagram of the readout system and a digital scope picture demonstrating operation of the electronics are presented in Fig. 2.

3. Results

The high-pressure ^{3}He scintillation detector (HeSD) was tested with an Am-Be neutron source with and without moderator (water bath or polyethylene moderator), and a ^{137}Cs gamma-ray source.

3.1. Detecting neutrons and gammas

A pulse height spectrum measured with the two-channel HeSD is shown in Fig.3. The figure shows a distribution of scintillation signals, each of which is the sum of two signals measured from two photodiodes. The HeSD was irradiated with neutrons from a 30 mCi Am-Be radioactive source. In Fig.3, a peak represents the thermal neutron absorption. The "horizontal" wing on the right-hand side of the peak represents elastic scattering fast neutrons. The moderator enriches the spectrum with thermal neutrons and the intensity of the peak increased when a neutron source is placed inside the moderator.

The LED peak is used for calibration purposes and allows estimation of the internal resolution of the photodiodes working in high-pressure ^{3}He. The value is about 8% FWHM, which is about the same as measured at normal conditions.

3.2. Position sensitivity

Two-dimensional distributions of individual signals measured in coincidence from two photodiodes are presented in Figures 4 and 5. The so-called "fish-tail" distribution (Fig.4) represents detection of thermal neutrons at different points of the between-photodiode gap filled with pressurized ^{3}He. Events close to APD1, for instance register higher on the APD1 axis, compared with the APD2 axis. The different concentration of events in the two fans of the tail is a result of the location of the neutron source on the APD1 side of the device for this experiment. The shape of the fishtail distribution represents position sensitivity of the detector to the location of neutron absorption points. Events squarely between the detectors with respect to their centers provide signals at position 0 in Fig. 6. Related events at the r = 0 position, or, on the Z-axis are oriented in a nearly straight line. Thus, for all events, the ratio of the two signals precisely determines the Z position for the event.

In order to estimate sensitivity of the detector to gamma rays, the detector was irradiated with a 662 keV gamma source. At the same gamma source intensity, the count rate from gamma rays was found to be a few order of magnitudes lower ($\sim 10^{-3}$) than from the neutrons (~1). Moreover, the 2D-distribution of gamma events has a completely different

configuration (Fig.5). Using location of the event in the 2D-plot, the rejection efficiency to gammas could be further improved by at least a factor of 10.

Efficiency of rejection events associated with direct interactions with photodiodes is demonstrated in the two plots in Fig.5.

3.3. Computer Simulations

The experimental data has been verified with computer simulations. Fig 7 shows the simulation result of a two-dimensional histogram of signals acquired from the two APDs activated with a point-like light source placed between the photodiodes. The plot confirms that the device has radial and depth spatial sensitivity as described in the previous section. The five families of the population represent virtual scans with light-emission points moving along the radius of the photodiodes on parallel planes located at five different depths between the photodiodes. The separation of the families illustrates the position sensing in the *Z* direction over the 7 mm gap between the photodiodes. The distribution points in one family represent the radial sensitivity along the 8-mm radius of the device. The "Fish-tail" distribution first observed in our experiments is fully reconstructed with this computer experiment.

The physical algorithm used in the computer simulations is a simplified physical model, in which the following assumptions and approximations are made:

- Index of refraction is 1 for the gas, 1.9 for the p-terphenyl layer, and 2 for the APD photodetector
- The p-terphenyl is set to be 100 percent absorbing scintillation light
- After being absorbed, the wave-shifted light is then re-emitted isotropically
- Every photon trajectory is adjusted at the two reflecting and refracting interfaces according to the classical laws of angular reflection and refraction.

4. Discussion

It was shown that:

- The high-pressure ^{3}He scintillation detectors can effectively detect thermal neutrons, fast neutrons, and, with high probability, distinguish the signals from both. There is developed a technology of high-pressure ^{3}He scintillation detectors (HeSD).
- Thermal and fast neutrons can be detected and counted separately with the same HeSD probe.
- The rejection ability for gamma rays of the same energy is about 10^{-4}.
- The HeSD could be constructed in configurations with or without moderator, or can be used for neutron imaging

The intensity of the natural gamma-ray background in the range of 764 keV has been measured to be about 60 counts per keV per NaI(Tl) kg per hour [10]. With ~5% FWHM energy resolution typical for photodetectors, the expected random count rate from natural

gamma-ray background will be about 50 counts per second. With coincidence selection of scintillations in the target gas, the background count rate could be suppressed to a level of about 10^{-2} counts per second. That is close to the count rate expected from the natural thermal neutron background.

A 0.1% xenon admixture into the target gas could absorb gamma-rays and generate scintillations. However, detection efficiency of the xenon admixture is about 10^{-6} at the energy range of interest. That makes this kind of background negligible.

Thermal neutrons may interact directly with the photodetectors. The screening effect from photodetectors will reduce the total detector sensitivity to the isotropic thermal neutron flux. However, using silicone thin photodiodes makes the effect negligible.

We see two possible applications of the detector. It can be used as a compact pocket-size individual neutron detector. Another approach is to use arrays of photodiodes for thermal neutron imaging similar to the scintillation gamma camera used with a solid scintillator for gamma ray imaging in nuclear medicine. Such detectors are required in neutron diffraction analyses.

Acknowledgements

The authors gratefully acknowledge the financial support of the Defense Threat Reduction Agency (DTRA), under contract DTRA01-99-C-0187. The authors would like to thank Dr. Anatoli Arodzero for his valuable contribution into investigation of scintillation properties of ^{3}He with photomultipliers at the first stage of the project and appreciate the support of Ed Knighton, Scott McPherson, and Leo Godbee in development of the instrumentation.

References

1. T.Aoyama e.a. NIM A314 (1992) 590-594
2. http://www.gepower.com/reuterstokes/oil_well/index.html
3. R.L.Schulte and M.Kesselman, NIM A422 (1999) 852-857
4. J.W. Leake, NIM 63 (1968) 329
5. http://lundlums.com/product/dets/m42-30.htm; http://www.eberline.com/instume/nrd.htm
6. http://www.inst.bnl.gov/GasDetectirLab/NeutronDetectors/Brochure/Overview.html
7. S. Belogurov e.a. 1995 IEEE NSS and MIC Record, v.1, p.519.
8. NIM A 283(1989)236
9. O.F. Nemets, Yu.V. Hoffman, "Nuclear Physics Hand-book" (in Russian), Naukova Dumka: Kiev, 1975, Table III.2. Ranges and stopping power of light ions.
10. A. Bolozdynya e.a. IEEE Trans. Nucl. Sci. 44 (1997)1046
11. G. Knoll, Radiation Detection and Measurements, 3rd edition, Jogn Wiley & Sons, 1999. P.557
12. A.E. Evans, Development of a high-pressure He-3 neutron scintillator spectrometer, Technical note LA-Q2TN-82-109, Los Alamos National Laboratory, April 29, 1982.
13. Nuclear Analysis Research and Development, LA-5889-PR Progress Report, UC-15, April 1975, pp.23-26.
14. U.S. patents ## 6,107,632; 6,100,530,; 6,075,261; 6,054,708; 6,011,266; 5,973,328; 5,940,460; 5,880,471; 5,880,469 …
15. http://www.pnl.gov/eshs/cap/ice/picpages/pic04.htm

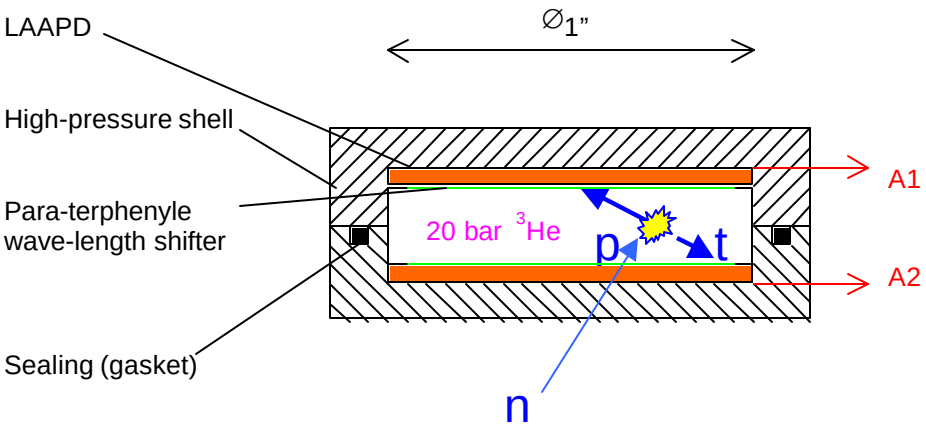

Fig.1. Two-channel He-3 scintillation detector with avalanche photodiode readout

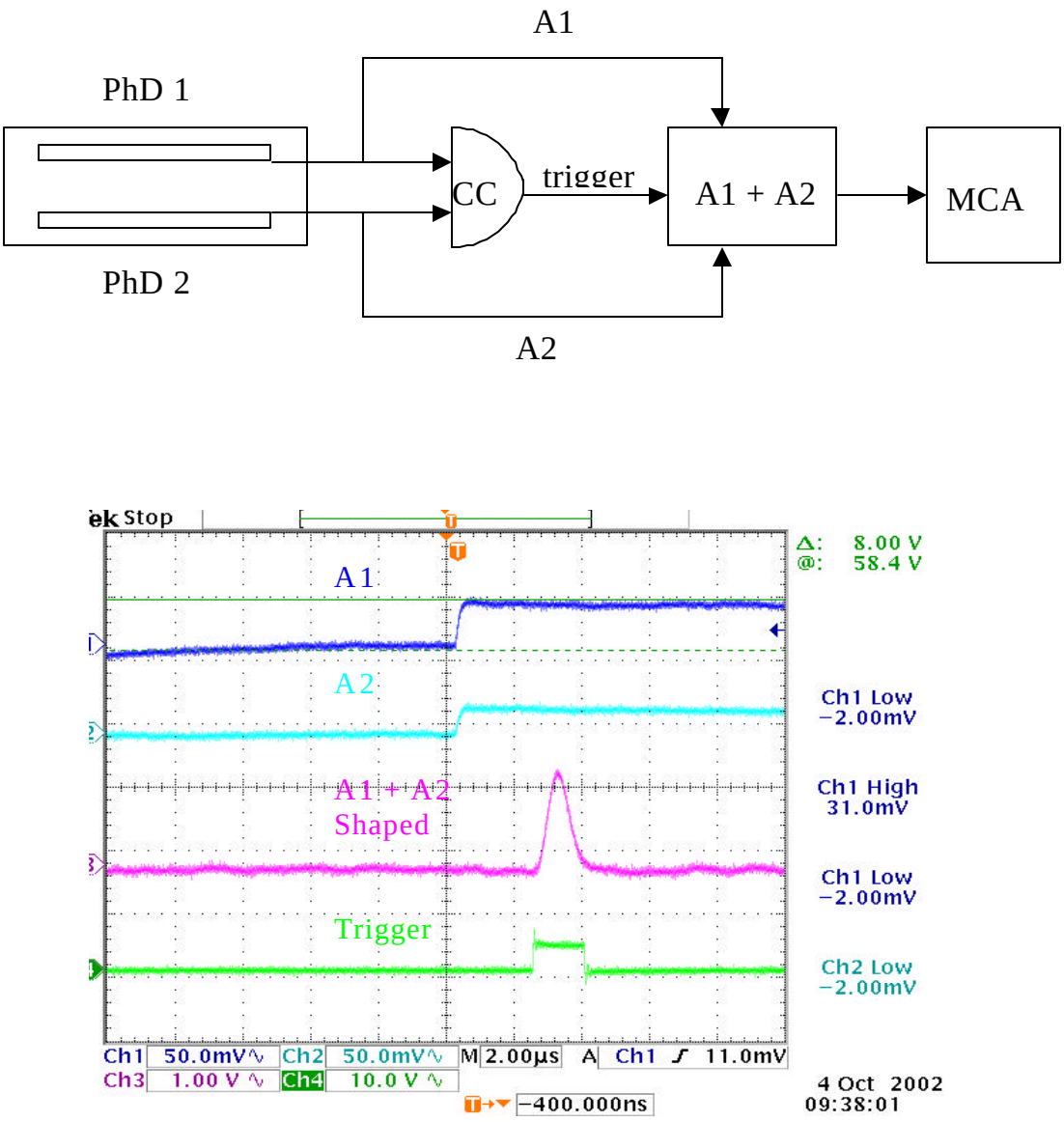

Figure 2 Block Diagram of a Data Acquisition System for 2-Channel HeSD in Coincidence Mode (top) and Digital Scope Picture (bottom)

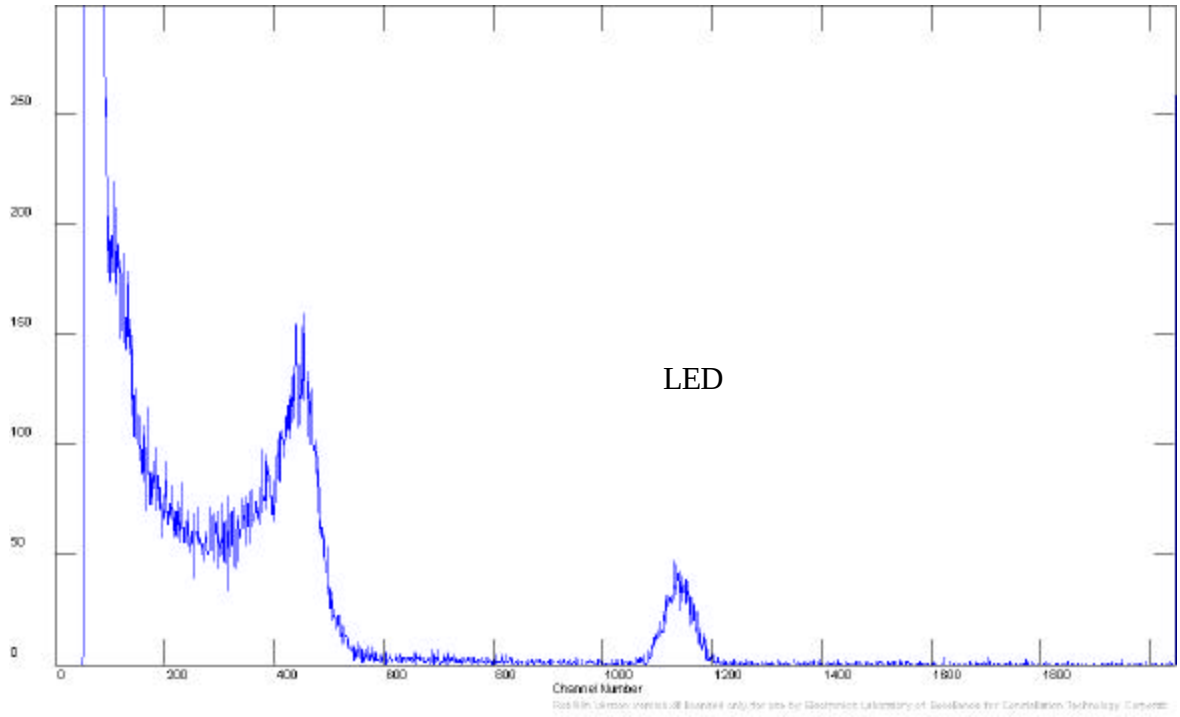

Figure 3. Pulse height spectrum of scintillations generated by thermal neutrons in 30 bar He-3 measured with two LAAPD photodiodes in coincidence

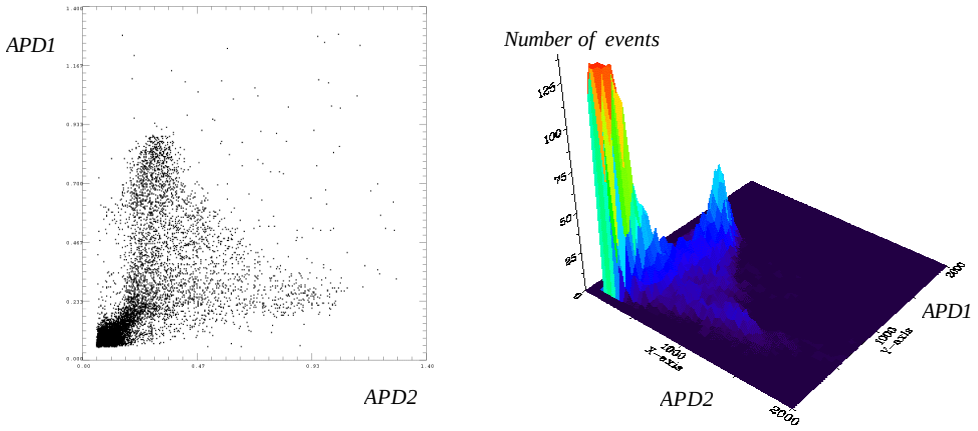

Figure 4. Plot of APD1 vs. APD2 signals generated by neutrons emitted from Am/Be source placed in water moderator

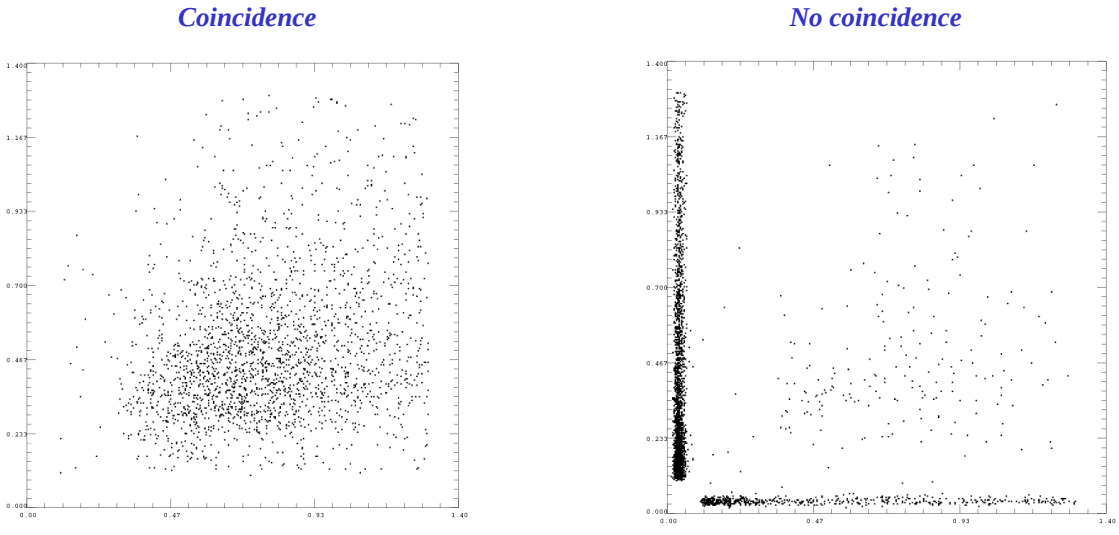

Figure 5. APD1 vs. APD2 137Cs gamma ray signals

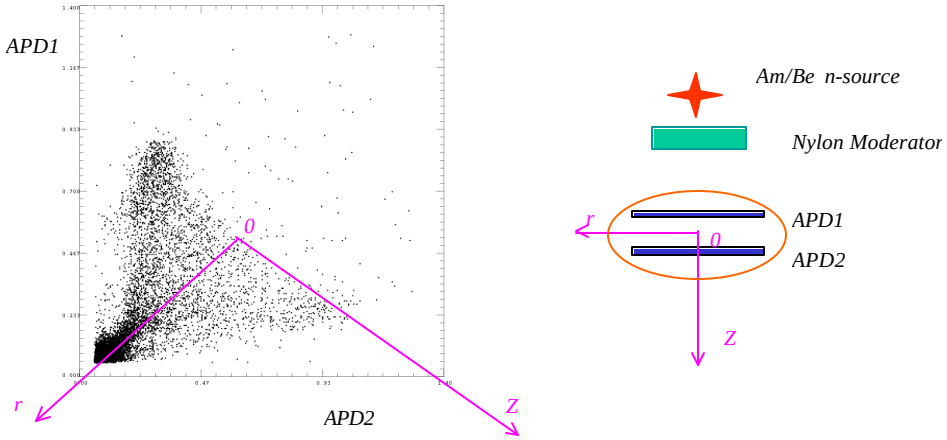

Figure 6. Position sensitivity of two-channel HeSD

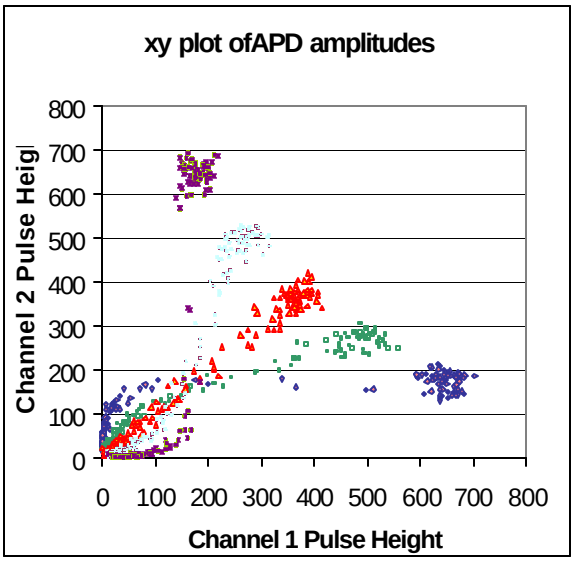

Figure 7. Computer simulation of two-dimensional distribution of scintillation signals acquired from two APDs in coincidence